A Fully Automated, Quasi-Optical, Rotary Polariser System for use at MM-Wavelengths

C.P.Unsworth* [+], J.C.G. Lesurf [+]

* The Department of Engineering Science, The University of Auckland,

70 Symond Street, Auckland 1003, New Zealand.

Email : c.unsworth@auckland.ac.nz

[+] The MM-Wave & High Field ESR group, School of Physics & Astronomy,

The University of St.Andrews, Fife, Scotland, KY16 9AJ, U.K.

Email : jcgl@st-and.ac.uk

Abstract

This article, describes the development of a fully automated rotary polariser quasi-optical system for use at millimetric frequencies. It is reported how the system can accurately measure the rotation and ellipticity that may be induced on a linearly polarised Gaussian Beam when it passes through a magnetic material under study with ~1% error. The system is demonstrated by the automatic characterisation of a plastoferrite sample in approximately 6 hrs using the 'Faraday Angle Resonance' method. This was a significant time saving over the conventional reflectance method which would take a skilled researcher ~ 1 week to perform. It is also reported how measurement of the 'Minor Faraday Angle' can produce more accurate results at mm-wavelengths.

1. Introduction

This article, describes how a fully automated rotary polariser quasi-optical system was developed for use at millimetric frequencies. It reports how the system was built, interfaced to several instruments, fully automated by computer control and the issues that were faced and overcome for use at mm-wavelengths. It is then demonstrated how the system can measure accurate rotation and ellipticity that may be induced on a linear polarised beam. The motivation of the work is concerned with the classification of ferrite materials in the manufacture of Freespace Faraday Rotators[1-3,23]. So the system is used to measure the variation in rotation and ellipticity that occurs with frequency when a linear polarised Gaussian beam interrogates a plastoferrite sample. Hence, the optimum thickness (L_{OPT}) of the ferrite necessary for 45^0 rotation is reported using the method of 'Faraday Angle Resonance' [4]. Conclusions of the work are then presented.

2. Experimental setup

Figure 1 shows the experimental setup of the fully automated system. Each part of the system is now described.

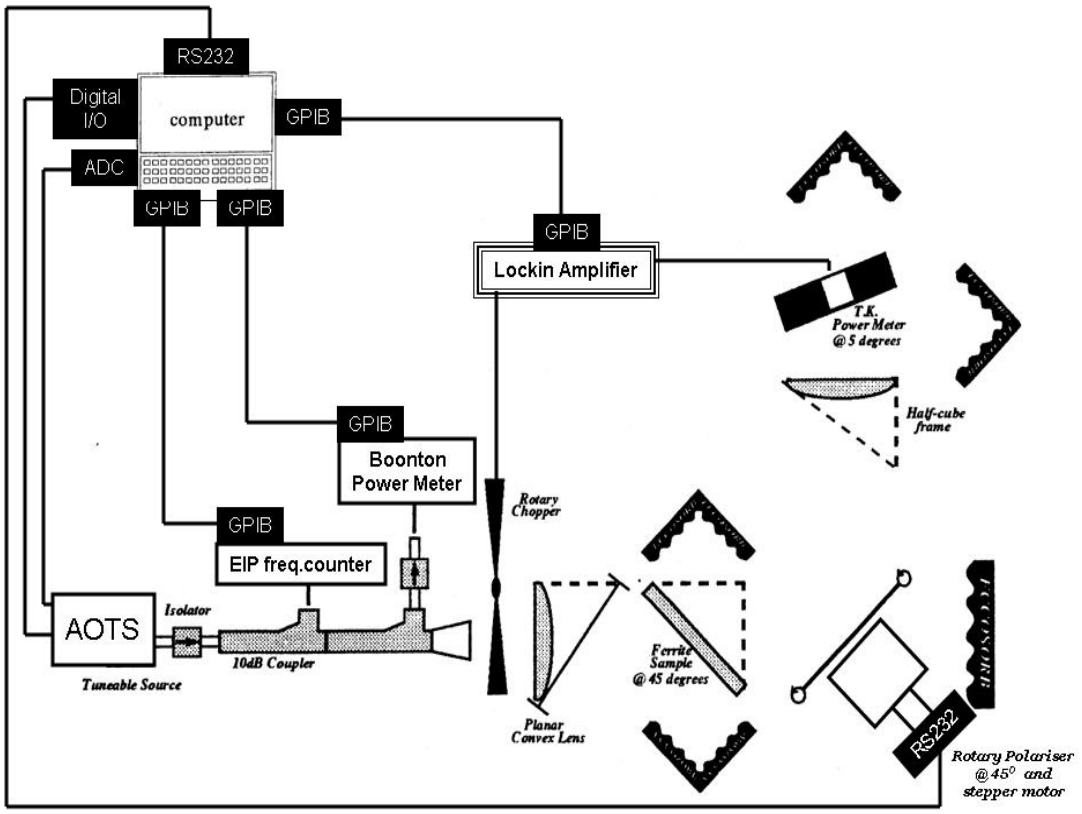

Figure 1 : The Fully Automated Rotary Polariser Quasi-Optical Setup

2.1 The Automatic Oscillator Tuning System (AOTS)

The 'Automated Oscillator Tuning System' (AOTS), developed in [5-6] is a piece of electronics that operates mechanical motors that were fixed to the frequency and backshort tuners of a coaxial cavity, resonant cap mm-wave oscillator [7]. By interfacing the AOTS to a computer, the frequency and power of the oscillator could be adjusted automatically by a computer program. Thus, the AOTS has wide functionality. The AOTS was used in the rotary polariser quasi-optical system to step through the dynamic frequency range of the mm-wave oscillator, at discrete intervals (up to 100MHz resolution) and then to adjust the backshort so as to maximise the oscillator's power at each frequency. A control program operated the AOTS and took readings of frequency and power of the oscillator from an EIP frequency counter [8] and

Boonton Power Meter [9] respectively. The computer used was an Acorn Archimedes Computer [10]. The interface from the computer to the AOTS was via a 'Wildvision Card' [10] which contained several digital I/O channels and ADC channels. All computer programs to control the AOTS and the rest of the system were written in the BBC Basic V [5].

2.2 Propagation of the Gaussian beam through the experimental setup

The mm-wave radiation produced by the oscillator propagated through a waveguide (W27) isolator [11], through two waveguide 10dB couplers [11], a further isolator and a feedhorn [11] which coupled it into freespace. The first 10dB coupler passed 90% of the radiation onto the next coupler and 10% to the EIP frequency counter. Similarly the second 10dB coupler passed 90% of the radiation onto the feedhorn and to freespace and 10% to a waveguide isolator which connected to the Boonton power meter. Both waveguide isolators served to protect both the source and the power meter from any reflections that could re-enter the waveguides and damage the devices.

The feedhorn propagated a vertically polarised mm-wave Gaussian beam [11] into freespace. The beam would be chopped by a mechanical rotary chopper, described in section 2.7, such that it could be detected later by a Thomas Keating (T.K) power meter, described in section 2.6. The beam was then focused by a high density polyethylene (H.D.P.E) planar convex lens [11] located within a half-cube [11] and through a horizontal polariser grid [11] which only passes a vertical polarisation. The beam would then propagate onto the magnetic sample or Faraday rotator [1-3] inclined at 45% located in a half-cube. However, any material under study could be placed here. The

vertically polarised beam would interact with the magnetic sample and be rotated through some angle (θ). In addition it could suffer some ellipticity if the material were anisotropic. The rotated beam then propagated towards the rotary polariser where it would form its beam waist. The rotary polariser, described in section 2.4, was controlled by the computer to move through a half revolution in 200 discrete steps. Only when the wires of the rotary polariser were parallel to the rotated beam would the full power of the beam be reflected towards the detector. Similarly, when the wires were orthogonal then the power would be dumped into the cavity of the rotary polariser and absorbed. Thus, powers ranging from zero to the maximum power within the beam would be reflected depending on the orientation of the wires of the rotary polariser. The reflected radiation would then pass to another planar convex lens located within a half-cube which would focus it to the pressure cell of the TK power meter. The Lockin Amplifier, described in section 2.8, would determine the voltage of the detector from the chopped signal and pass this to the computer. A control program [5] was implemented to automatically perform the above mentioned experiment on a magnetic sample.

2.3 Reducing Standing Waves within the Experimental Setup

Reflections from any optical component within the system whose plane is perpendicular to the direction of propagation of the radiation could create standing waves [11]. By careful planning in the design of the optical system, standing waves could be greatly reduced or eliminated. This is now explained. The implementation of planar convex lenses into the system as shown in Figure 1, served to reduce standing waves. If one considers the rapidly

expanding gaussian beam that propagates from the source feedhorn toward the planar side of the lens. Any reflection from the planar face will not be channeled back into the feed, as with a convex lens, but rather diffracted in a different manner out of the system, described by [12]. In addition, the lenses were ‘blazed’ [12] which allows the radiation to couple into the lens more efficiently and hence minimise reflections. Reflections from the rotary chopper blades back to the source are dealt with the waveguide isolator. Similarly, reflections towards the Boonton detector are also dissipated with a waveguide isolator. As the Gaussian beam propagates toward the unmatched ferrite sample reflections will occur. Angling the sample at 45° will divert any reflection from the sample toward the ‘Radar absorbent material’ R.A.M. (manufactured by Eccosorb [13]) and out of the system. Similarly, if the beam propagates through the sample, but is then reflected from the convex face of the 2nd lens back toward the ferrite, it too is diverted to the R.A.M and absorbed. By angling the TK meter at 5° to the incoming radiation reflections are diverted whilst preserving the polarisation insensitivity necessary to detect an arbitrary polarisation reflected from the rotary polariser. The cavity of the rotary polariser, described in section 2.4, was also designed to dump any stray reflections to R.A.M. rather than allowing them to re-enter the quasi-optical system. Although the blazing of the lenses should minimise reflections from the lens surfaces, reflections between the convex surfaces of the lenses and the rotary polariser wires can also exist. Standing waves created from these reflections could not be avoided. In addition we suggest how measurement of the ‘Minor Faraday Angle’, defined in section 4, may further serve to reduce reflection in the system.

2.4 The Rotary Polariser

A rotary polariser was developed to the design shown in Figure 2. A wire grid polariser was constructed on a circular aluminum frame. The frame was held in 3 equally spaced positions by aluminum rods, 100mm in length. These were attached to a wheel-like frame. The wheel-like frame was connected to a cylindrical hub. The hub passed through an aluminum housing unit. The hub could rotate freely within the housing unit because of bearing rings located within the housing unit. A stepper-motor was affixed to the back of the housing unit. This was a S83-135, size 34 motor driven by a PDX15 single-axis mini-step drive [5,14]. The shaft of the stepper-motor was fixed rigidly within the hub. The housing unit served to support the whole system and could be located on a baseplate[11]. Thus, it was possible for the stepper-motor to turn the polariser through discrete steps. The polariser, rods and wheel-like frame formed an open cavity structure.

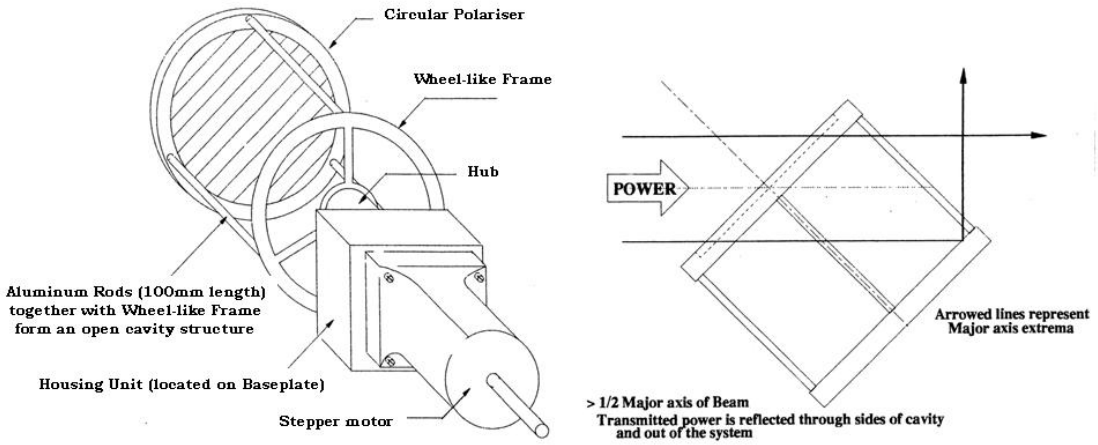

Figure 2 : The Rotary Polariser & Open Cavity Design

The open cavity structure was developed for two reasons. The first was to reduce the inertia of the system. The second reason was to allow for any

power that was transmitted through the polariser to be reflected from the back of the cavity out of the sides of the instrument and thus out of the experimental setup, shown in Figure 2.

It was determined that that as long as the cavity length was greater than half the radius of the Gaussian beam then any power would be reflected out the system. This corresponds to half the major axis of the beam since the instrument was angled at 45^0 to the incoming radiation. For this application it was determined that 63mm was the minimum cavity length necessary. For an extra safeguard, the cavity length was chosen to be 100mm and the back of the cavity was affixed with 20dB of R.A.M. The stepper-motor of the rotary polariser system was RS232 compatible and thus interfaced via an RS232 port of the computer. The detailed design of the rotary polariser and its operation can be found in [5].

2.5 Relationship Between Seen Angle (χ) & Actual Angle (θ)

Since the rotary polariser was inclined at 45^0 to the input beam, the angle of the polariser wires, as “Seen” by the input radiation would appear different to that of the actual angle of the wires if viewed at normal incidence. Because of this, the radiation reflected to the detectors would be inclined at the "Seen Angle". A relationship between the "Seen Angle” (χ), "Actual Angle” (θ) and inclination angle ($\varepsilon = 45^0$) of the rotary polariser to the radiation was determined and is highlighted in Figure 3.

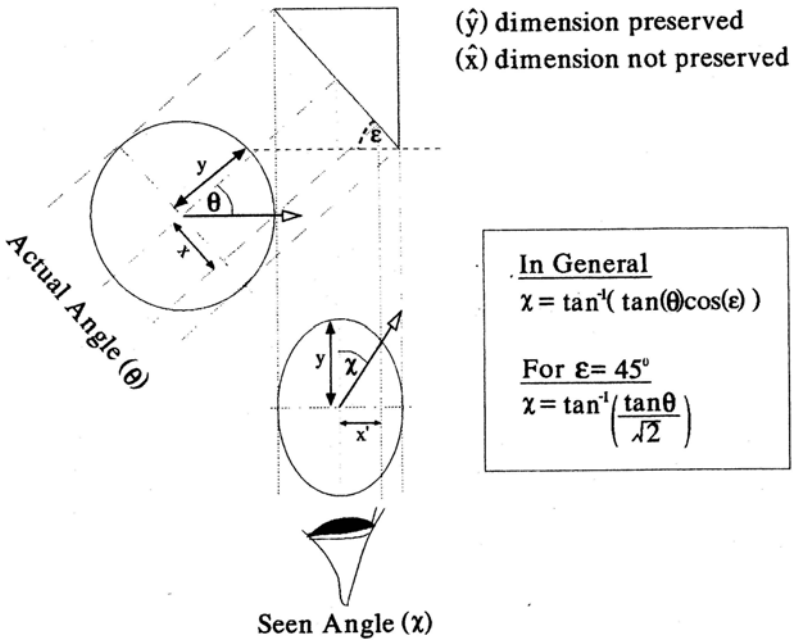

Figure 3 : Relationship between Seen, Actual and Inclination Angle

Thus, as the rotary polariser was stepped through 180^0, the radiation from the polariser wires would be reflected by the seen angle.

2.6 The Thomas Keating (TK) Free-space power meter

The Thomas Keating (TK) Freespace Power Meter was the detector used in the automated system [15]. The detector consisted of a closed air filled cell into which a thin metal film of an area $30mm^2$ was located. The TK meter detects the incident radiation as follows. When an amplitude modulated signal falls upon the cell, approximately 50% of the radiation is absorbed by the thin metal film. The other 50% is either reflected from or transmitted through the cell. The power absorbed, heats the metal film and changes the air pressure within the closed cell. The pressure change of the cell is closely proportional to the power of the incident beam. A pressure transducer monitors the change in pressure of the cell when the beam is amplitude modulated. Hence an A.C.

voltage is output from the power meter which can be used to determine the amount of power in the incident beam.

The amount of reflection/transmission from/through the cell is dependent on the orientation of the TK with respect to the incident radiation. When the TK meter is oriented at 55°, known as the Brewster Angle [16], to the incident radiation there is no reflection from the cell. Instead the radiation is not absorbed but transmitted through the cell. At the Brewster angle the TK voltage output is frequency independent. However, at the Brewster angle the TK is sensitive only to a vertically polarised input. At angles other than the Brewster angle the TK becomes insensitive to the polarisation of the radiation and its voltage output is frequency dependent. In addition, if the TK meter is positioned at normal incidence to the radiation then it becomes equally sensitive to all polarisations. Since, the rotary polariser would be reflecting arbitrary polarisations toward the TK, near normal incidence was suitable for this application.

It was found by angling the TK at near normal incidence (~ 5°) to the beam was sufficient for detection of arbitrary polarisations and also allowed for standing waves within the system to be minimised. The TK was positioned at this angle and at a distance of 87mm from the 2nd lens. This was the calculated in [5] as the optimum distance that gave a beam-width of no greater than 5.83mm over W-band at the detector's face. With the TK angled at 5°, an elliptical shaped beam with major axis 5.85mm and minor axis of 5.83mm would be projected onto the TK's face. This was easily contained within the 30mm^2 pressure cell of the TK

Due to the TK being inclined at 5° to the incoming radiation, the seen angle reflected from the rotary polariser would not be the same as the angle detected at the TK. Thus, a further correction was made in a similar fashion to the correction made for the seen angle. From herein, the seen angle incorporates the correction made for the detected angle of the T.K also.

2.7 The Mechanical Chopper

In order for the TK to operate correctly it was necessary for the incident beam to be modulated in amplitude. This was achieved by placing a rotary bladed shutter, or mechanical chopper, in front of the feedhorn in the path of the propagating beam. The chopper consisted of three blades of the same area made from aluminum and coated with (R.A.M). The blades were separated from each other by an area of freespace equal to the area of a blade. Therefore, as the chopper rotated the continuous wave signal from the source, would be completely absorbed when a blade was in-front of the source and allowed to propagate into the experimental setup otherwise. Thus, the TK would receive a mechanically 'chopped' amplitude modulated signal. A small light tachometer attached to the chopper and connected to a small electronics unit was used to output a reference voltage. The reference voltage corresponded to the rate at which the source was being chopped. Square wave modulation was observed when the output voltage was connected to an oscilloscope. The modulation rate could then be adjusted by altering the voltage supplied to the motor of the chopper. A modulation rate of 20-40Hz was suggested in the operating manual of the TK, as a maximum signal-to-

noise ratio is obtained in this range. Hence, a modulation rate of 30Hz was chosen.

2.8 The Lockin Amplifier

An EG&G Princeton Applied Research 5210 Lockin Amplifier [17] was employed to interface the T .K. to the computer [10]. As well as interfacing the TK to the computer the Lockin Amplifier also gave one the opportunity to perform phase-sensitive detection [17] on the input signal. Phase-sensitive detection was achieved by connecting the AC output from the TK to the signal channel of the Lockin and connecting the AC reference voltage from the mechanical chopper to the Lockin's reference channel. In this manner, DC drift could be eliminated and a high rejection of frequencies outside the chopping frequency of the source was attained by adjustment of the time constant of the Lockin Amplifier. A large time constant, of 3secs, would give a very high rejection of frequencies and suppress noise well. However, this would mean that at least a 3 second delay would be necessary every time the input signal changed significantly. The input signal could be expected to change significantly every time the stepper moved through one step. As a rule of thumb, it is good practice to allow for at least 3 time constants to pass before taking a measurement. Because of the large amount of discrete steps the rotary polariser would perform, namely 200 steps in half a revolution, a time of around 30 minutes would be required. In addition, this is assumes only a single measurement per step is being made and that no other instrument is being read. In order to reduce the time of an experiment, it was decided to use a time constant of 3ms which would give the order of ~1 second before

measurements were taken. This is short enough as reduce experimental time whilst also allowing for approximately 3 time constants to pass, hence suppressing noise. The Lockin Amplifier was ‘General Purpose Interface Bus’ (GPIB) compatible [18]. Hence, it was interfaced to the computer [10] and operated via a control program detailed in [5].

3. Measurement of the TK voltage

A series of computer procedures were written to determine the voltage from the TK meter, detailed in [5]. Because of the possible drift that could occur in the mm-wave oscillator’s power, it was necessary to normalize the voltage received from the TK to the power of the mm-wave source, as read from the GPIB compatible Boonton power meter [9]. This was termed the 'corrected voltage'. Five readings from the Lockin and Boonton were made and averaged to reduce noise in the system and approximate the signal accurately. Figure 4, shows a typical experimental run consisting of half a revolution. This produces a smooth voltage response from the TK using the method described.

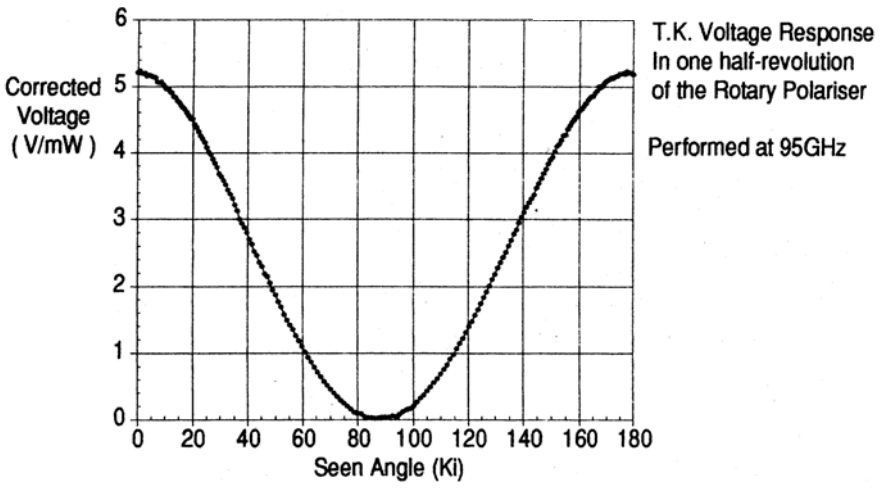

Figure 4 : Response of TK for half a revolution of the rotary polariser

4. Measuring the Faraday Angle & Ellipticity of a Gaussian Beam

Although the TK is only sensitive to the vertical polarisation state when at the Brewster angle, the voltage output for various power input remains the same for all frequencies. Thus, the TK's Detectivity (D^*), is said to be frequency independent. When one angles the TK away from the Brewster angle, it becomes receptive to arbitrary polarised inputs but its detectivity becomes frequency dependent. Since this application was only concerned with measuring accurate rotated angles, due to the Faraday effect [1], the frequency dependency of the TK's detectivity was not an issue. It was not an issue because although the detectivity was frequency dependent, the voltages from the TK at spot frequencies would remain relative to one another. The voltage would also be proportional to the power detected by the TK. Hence, the largest voltage obtained will represent the largest power output. In relation to the Faraday angle, if a linear polarised beam were input into the system a maximum voltage would correspond to the position at which the Faraday Angle existed. If the magnetic sample had distorted the original linear polarised beam to produce an elliptically polarised beam, then the maximum voltage would represent the proportion of power in the major axis of the beam. Similarly, a minimum voltage would represent the proportion of power in the minor axis of the beam. This minimum voltage would also occur 90° away from the Faraday Angle. Therefore, by observing the maximum and minimum voltages one could define the ellipticity of the beam. From herein, the position at which the maximum voltage occurs will be referred to as the 'Major Faraday Angle' and the position at which the minimum voltage occurs will be referred to as the 'Minor Faraday Angle'. Thus, it was important to locate both the

Major and Minor Faraday Angles and also to measure the voltage at each of these locations to determine the ellipticity of the beam.

Prior to this work, a semi-automated prototype of the above system, with a different detection scheme was developed, described in [5]. The semi-automated version incorporated a Martin-Puplett interferometer [11] into its setup which allowed for different ellipticities of the beam to be created and measured using the rotary polariser. It was found by defining the ellipticity as :

$$\text{Ellipticity} = (\text{Maximum Voltage} / \text{Minimum Voltage}) \quad \ldots.1)$$

Then various beam shapes could be identified. From the definition described in equation 1) it was found that when :

Ellipticity = 0 → (Linear Polarised Beam),
Minima located on x-axis

0<Ellipticity<1 → (Elliptical Polarised Beam),
Major axis at maxima, Minor axis at minima

Ellipticity = 1 → (Circular Polarised Beam),
Equal power distribution, major=minor axis

Figure 5, highlights the results from the prototype system for different ellipticities.

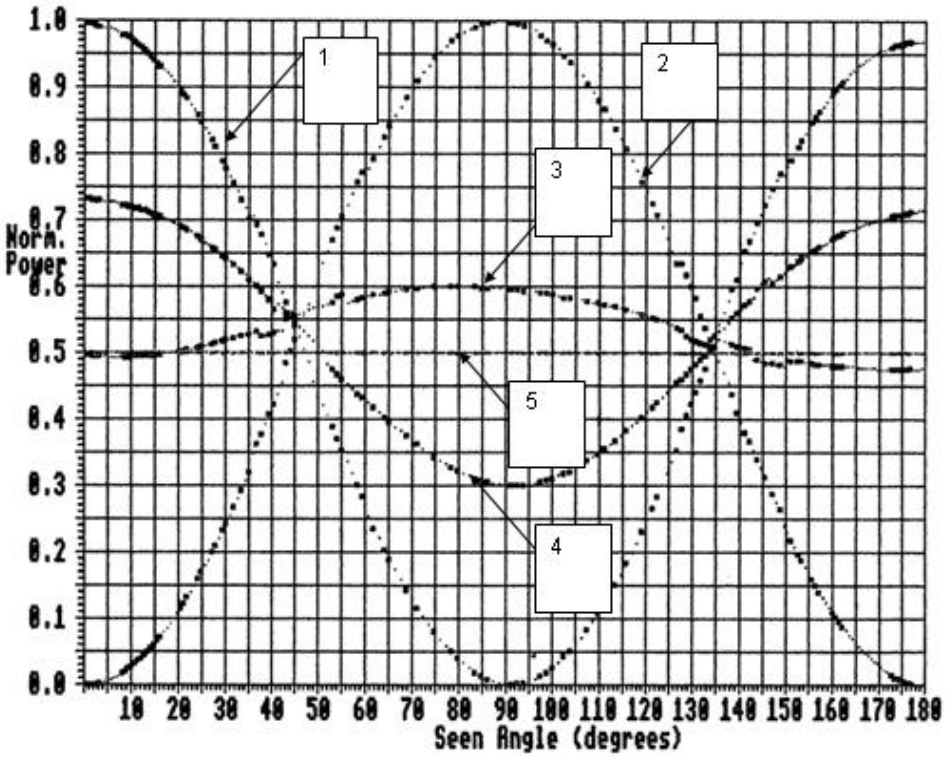

Figure 5 : Polarisation Measurements

Table 1, highlights the ellipticities measured from the results displayed in Figure 5. As one can see the linear polarisation will always have its maximum or minimum powers at unity and zero for horizontal polarisation which would become reversed for vertical polarisation. Circular polarisation always appears as a straight line (or DC offset) with no maximum or minimum angle discernable. Finally, an elliptical polarised beam will have distinct maximum and minimum powers.

Data set	Max. norm Power	Max. Seen Angle ^{0}	Min. norm power	Min. Seen Angle ^{0}	Ellipticity
1	0.997	1.3	0.002	91.3	0 (Horiz pol)
2	0.731	0	0.003	92.6	0.41 (Ellip pol)
3	0.602	79.9	0.476	174.9	0.79 (Ellip pol)
4	1.000	88.7	0.0008	0	0 (Vert pol)
5	0.5	0	0.5	0	1 (Circ. Pol)

Table 1 : Tabulated results corresponding to Figure 5

The prototype system was used to demonstrate how ellipticity could be measured. However, one can see that the difference between the maximum and minimum seen angle was not always 90^0 exactly. This was due to noise effects in the system. In the fully automated system, as will be described later, such inaccuracies were reduced using a least squares parabola fit, described later in section 6.

5. Reducing Experimental time

In a typical experiment, it would required for one to measure the behavior of the ellipticity or major and minor Faraday angles of a material across W-band. This would mean that the system would have to perform these measurements for every frequency. It was found to take ~10 minutes to perform measurements for a full half-revolution (consisting of 200 discrete steps).

Then to execute a full half-revolution for every discrete frequency, namely with frequency increments of 100MHz using the AOTS, could take a staggering 30+ hrs for a single sample. In order to reduce, the experimental time it was acknowledged that half-revolution was only required once at the beginning of the experiment. This was to establish the positions of the major and minor Faraday angle. Once the major and minor Faraday angles were identified, one could simply track about their known positions as the frequency was incremented. Since the frequency increment was to be small, 100-200MHz, the change in the Faraday angle would also be small. It was found, by tracking ±10 degrees, (±10 discrete steps) either side of the major and minor Faraday angles, one would encounter the new position of the major/minor Faraday angle. A tracking procedure was implemented in code and found to successfully reduce the experimental time to that of ~6hrs. This reduction was significant in comparison to the conventional reflectance method used to characterise ferrite materials, documented in [5]. Since the reflectance method would require up to 1 week of manual work, requiring multiple experiments on several samples of the material under study.

6. Prediction of the Major & Minor Faraday Angles over Thermal, Accoustic/Vibrational Noise Fluctuations.

The only instrument to be radically effected by noise was the TK Whilst the TK offered highly sensitive wideband detection it was also sensitive to a wideband noise and could detect changes in temperature and accoustic/vibrational effects [15]. Thus, the TK's thermal and accoustic/vibrational noise fluctuations were found to occur randomly on the

major/minor Faraday angles which could lead to inaccurate measurement.

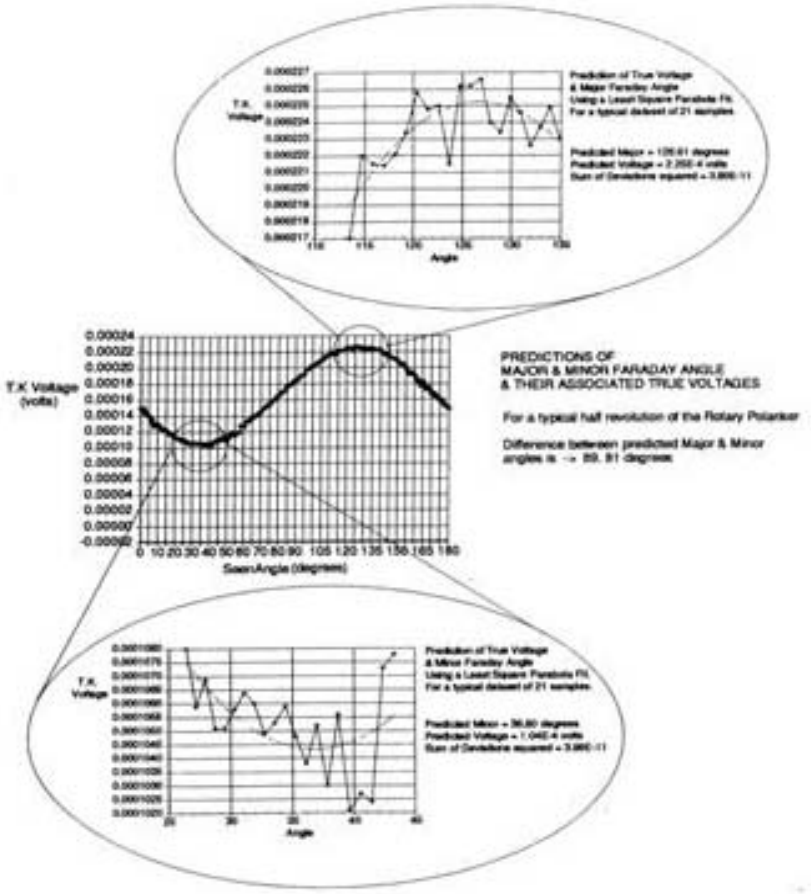

Figure 6 : Use of a least squares parabola fit to cut through the noise floor

By acknowledging that the distribution of data points around the areas of interest, namely the major/minor Faraday angles, were parabolic in shape, one could fit a least squares parabola around the area of interest. Hence, one could cut through the noise floor to determine the major and minor Faraday angles accurately and also determine the true TK voltages which were used to accurately calculate the ellipticity of the beam, described in detail in [5] and shown in Figure 6.

7. Results For Sample 11.

Sample 11 consisted of 'Polycrystalline, uni-axial, anisotropic Strontium Hexaferrite' with a 'Magnetoplumbite' structure (SrM)[20,21] whose pulverised powdered form was embedded in a low loss polymer matrix to create a composite semi-anisotropic plastoferrite. Two $100mm^2$ pieces of this material were affixed together using a thinned glue to form sample 11. The material had been cut at 22.5° to its magnetic flux lines, described in [5]. The actual thickness of sample 11 was 3.05mm which gave an optical thickness of 4.31mm at 45^0. Figure 7, highlights the results using the fully automated system presented here. The upper plot is a plot of the Major Faraday Angle with frequency. The middle plot is a plot of the Minor Faraday angle versus frequency and the lower plot is a measure of the ellipticity of the beam with frequency. All the plots were performed over the 83-100GHz region with 100MHz frequency increments.

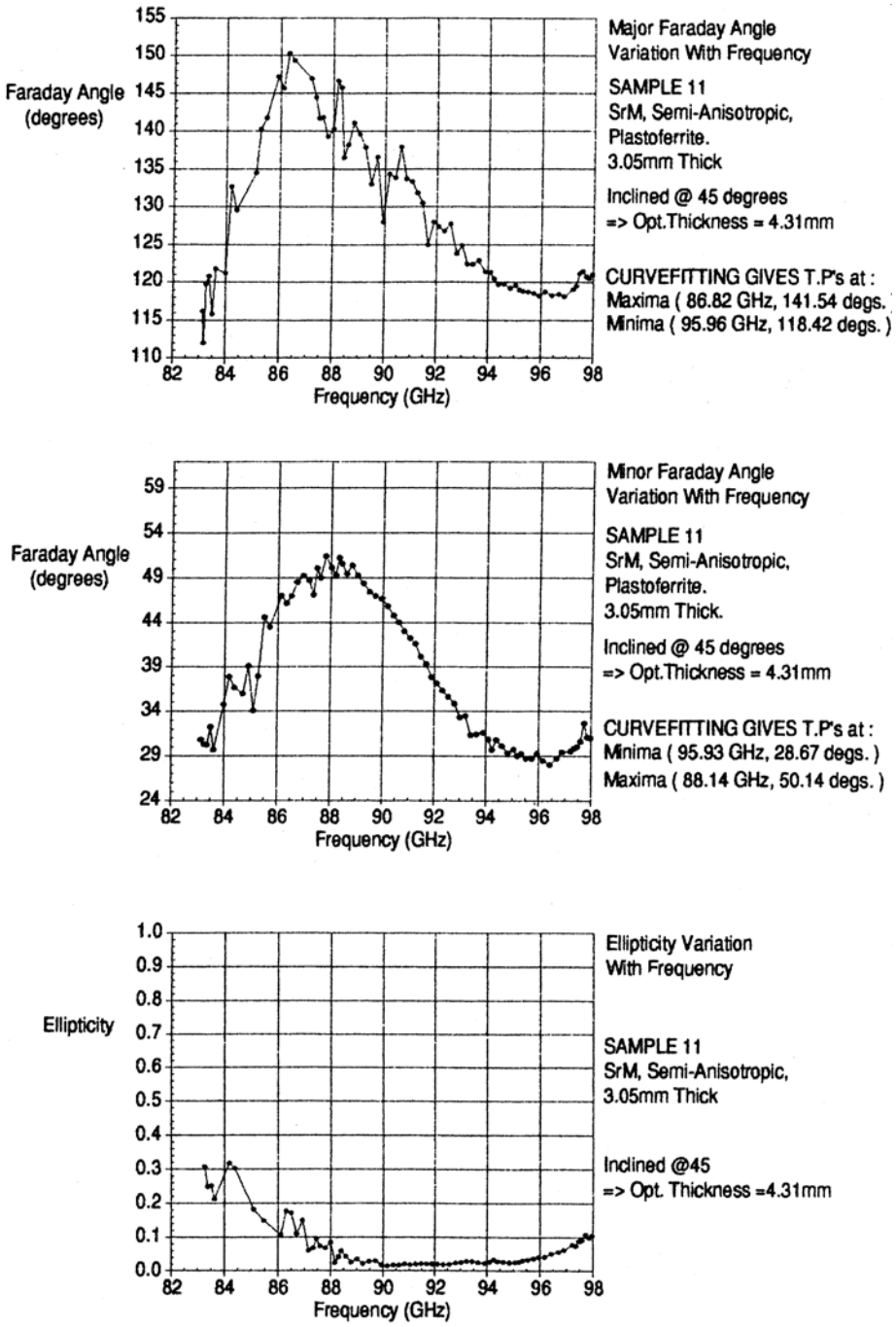

Figure 7 : Major, Minor Faraday Angle and ellipticity variation with frequency for Sample 11

7.1. Results Analysis for Sample 11

The sinusoidal 'Faraday Angle Resonance' trait observed by Raum [4] is

evident in the upper and middle plots of Figure 7. The erratic nature of the Major Faraday Angle plot is likely to be heightened since the sample consisted of two pieces. The Major Faraday Angle also contains a very large portion of the power, producing a greater likelihood of multiple reflections occurring between each of the two pieces of ferrite and introducing further rotational effects.

One strong conclusion that can be drawn from these experiments is that the 'Minor Faraday Angle' plot is much smoother than the Major Faraday Angle plot. This is because the Minor Faraday Angle contains very little power compared to the Major Faraday Angle. This is because the Minor Faraday Angle is effectively a null measurement since all the power should be dumped into the cavity at this angle. For this reason, we suggest that the Minor Faraday angle be used in preference to the Major Faraday angle for Faraday Angle Resonance measurements at millimeter wavelengths. The lower plot shows that the beam is linearly polarised over 90-94GHz and small ellipticity effects start to creep in > 94GHz and larger ellipticities are observed at 83-88GHz. These are probably due to the multi-path reflections becoming more dominant between the two pieces of affixed ferrite at these frequencies. The ellipticity measurement is used in [22] to further characterise Faraday Rotators at mm-wavelengths.

The parabolic curve-fit, described in section 6, was then applied again to the range of points around the maxima and minima features of the upper and middle plots. Using this method it was possible to locate very accurately the true positions of the major and minor Faraday angle. The results from the curve-fit are tabulated in Table 2.

Type of Turning point	Major Faraday Angle	Minor Faraday Angle
Maximum T.P,	(86.82 GHz, 141.54°)	(88.14 GHz, 50.14°)
Minima T.P.	(95.96 GHz, 118.42°)	(95.93 GHz, 28.67°)

Table 2 : Major & Minor Faraday Angle locations for Sample 11

The maxima turning points of both the major and minor Faraday angles should be located at the same frequency and should also occur 90° apart. From the curve-fitted results this is almost exact with ≈ 2% error. It was found that the minima turning points had a < 1% deviation. An accurate value for the Major Faraday Angle and its corresponding frequency is necessary to make a good prediction of ($\Delta\varphi$) which is the rotation/single pass [4]. By averaging the maxima turning points of the major and minor Faraday angle and similarly for the minima turning points, even better estimate of the turning points can be made for the maxima and minima of the Major Faraday Angle plots. The averages are shown in Table 3.

Type of Turning Point	Major Faraday Angle
Averaged Maxima ($\Delta\varphi_{MAX}$)	(87.48 GHz, 140.84°)
Averaged Minima ($\Delta\varphi_{MIN}$)	(95.95 GHz, 118.55°)

Table 3 : Averaged Faraday Angles for Sample 11

Substituting for ($\Delta\varphi_{MAX}$) and ($\Delta\varphi_{MIN}$) in equation 1) and 2) the amount of rotation incurred upon a single pass through an optical thickness of 4.31mm of Sample 11 was found to be :

$$\Delta\varphi = 50° 44' / \text{single pass}$$

$$= 11 ° 46' / \text{mm}$$

Therefore, for 45° rotation over the region (87.48 - 95.95GHz) a sample with an optical thickness 3.82mm would be required. Translating this back to the actual thickness gives 2.70mm. However, this is for a sample inclined at 45°. Conventional reflectance measurements made on the same sample predicted a thickness of ~2.75mm [5]. These were when the sample had its plane perpendicular to the incident radiation. Therefore, the figure determined appears to be an overestimate. However, this is not the case as two additional effects are occurring due to the angling of the sample. Although, angling the ferrite at 45° prevents standing waves in the experimental setup, it also angles the c-axis and thus the internal biassing field of the sample by 45°. This means that the incident radiation will see an effective component of the anisotropy field which is a factor $\sqrt{2}$ smaller in magnitude. The smaller field will serve to rotate the incident radiation less and hence a larger thickness is to be expected to attain 45° rotation. In addition, there also exists a field component which is perpendicular to the direction of propagation of the beam. This affects the incident beam, described by the Cotton-Mouton Effect [19]. This effect is related to the Faraday Effect, but the rotation incurred upon the beam is smaller in comparison. Hence, the angling of the ferrite serves to reduce the rotation incurred upon the beam. Thus, the results determined here are for ferrites angled at 45^0 to the incident radiation.

Conclusions

This article, reports the development of a fully automated rotary polariser quasi-optical system for millimetric frequencies. It has been demonstrated how the system can accurately measure the rotation of a linear polarised Gaussian Beam from a ferrite sample and Faraday Rotator. In addition, it has been shown how the system can be used to measure the ellipticity of a Gaussian beam and hence measure any distortion that may be incurred upon a linear polarised beam with an error of ~1%. It has been shown how the system can be used to automatically characterise a magnetic sample in approximately 6 hrs using the Faraday Angle Resonance method. This is significant time saving over the conventional Reflectance method which would take a skilled researcher ~ 1 week to characterise. In addition, it was shown that tracking of the Minor Faraday Angle as opposed to the Major Faraday angle produces more accurate results .

Acknowledgements

The authors would like to thank Dr. D.A. Robertson and Dr. G.M. Smith from the MM-Wave & High Field ESR group at the University of St.Andrews, Scotland, for their help and advice during this work.

References

[1] G.F.Dionne, J.A.Weiss, G.A.Allen, W.D.Fitzgerald.: ‘A Quasi-Optical Ferrite Rotator For Millimeter Waves’, 1988, MTT Conference Symposium Digest, pp. 127-130.

[2] Smith G.M, Unsworth C.P, Webb M.R, Lesurf J.C.G.: 'Design, Analysis & Application Of High Performance, Permanently Magnetised, Quasi-Optical Faraday Rotators', IEEE MTT-S 1994 International Microwave Symposium, San Diego, USA, 1994, pp 293-296.

[3] Unsworth C.P. , Smith G.M, Kang S, Puplett E, Franklin D, Lesurf J.C.G.: 'Microwave, Millimeter Wave & Submillimeter Wave Free-Space Faraday Rotators', IEEE MTT-S 1995 International Microwave Symposium, Orlando, USA, 1995, pp.1665-1668.

[4] M. Raum, 'Quasi-Optical Measurement Of Ferrite Parameters At Terahertz Frequencies By A New Method - Faraday Angle Resonance', International Journal Of Infrared & Millimeter Waves, 1994, Vol.15, No.7, pp.1211-1227.

[5] C. P. Unsworth.: 'A Fully Automated Millimetric Rotary Polariser Quasi-Optical System', PhD Thesis, 1997.

[6] C.P.Unsworth, J.C.G. Lesurf.: 'An Automated Oscillator Tuning System for Gunn Oscillator Characterisation at MM-Wavelengths', submitted to IEE Proceedings - Microwaves, Antennas and Propagation, June 06.

[7] G.M. Smith.: 'Transferred Electron Oscillators at MM Wave Frequencies and their Characterisation using Quasi-Optical Techniques', PhD Thesis, 1990.

[8] EIP Microwave Inc. 575 & 578 Source Locking Microwave Counters Manual, Sect. 10, pp.06-1 to 06-7.

[9] Boonton Electronics Corporation Instruction Manual for Model 4220 RF Power Meter, pgs. 4-13 to 4-23.

[10] http://www.acorncomputers.co.uk/, Accessed June 2006

[11] Lesurf, J.C.G.: 'Millimetre-wave Optics, Devices & Systems' , Adam Hilger-IOP Publishing, 1990.

[12], Harvey A.R.: 'A Millimeter Wave, Quasi-Optical Complex Impedance Bridge', PhD Thesis, The University of St.Andrews, 1990.

[13] Eccosorb is the registered trademark of Emerson & Cuming Microwave products, http://www.eccosorb.com/, Accessed June 2006.

[14] Manufactured by Compumotor & Digiplan, http://www.compumotor.com/, Accessed June 2006.

[15] The Thomas Keating Sub-millimeter Power Meter - PM104 Operating Manual, also http://qmciworks.ph.qmw.ac.uk/TKI/tkins.html, Accessed June 2006

[16] E.Hecht, 'Optics', Addison & Wesley Publishers, (2nd Edition, 1987), pp285.

[17] The EG&G Princeton Applied Research Model 5210 Lockin-Amplifier Instruction Manual.

[18] http://www.ni.com/gpib/, Accessed June 2006.

[19] D. Jiles.: 'An Introduction to Magnetism & Magnetic Materials', Chapman & Hall, 1991, pg 57.

[20] J.J.Went..: 'Ferroxdure - A Clan Of New Permanent Magnet Materials', Philips Tech.Rev., 13[7], 1952, pp.194-208,

[21] A.L. Stuijts, G.W.Rathenau, G.H.Weber.: 'Ferroxdure II & III - Anisotropic Permanent Magnet Materials', Philips Tech.Rev., 1954, 16 [5-6], pg.141.

[22] C.P.Unsworth, J.C.G Lesurf.: 'Observation of Frequency Dependent Faraday Angle Resonance in Ferrites & New Ellipticity Characterisation of

Freespace Faraday Rotators at MM-wavelengths', submitted to IEE Proceedings - Microwaves, Antennas and Propagation, June 2006.

[23] Hunter RI, Robertson DA, Goy P, Smith GM.: 'Large area W-band quasi-optical faraday rotators for imaging applications' The Joint 30th International Conference on Infrared and Millimeter Waves, IEEE. Part vol. 1, 2005, pp. 275-6, Piscataway, NJ, USA.